

This article was downloaded by:

On: 21 January 2011

Access details: *Access Details: Free Access*

Publisher *Taylor & Francis*

Informa Ltd Registered in England and Wales Registered Number: 1072954 Registered office: Mortimer House, 37-41 Mortimer Street, London W1T 3JH, UK



The Journal of Adhesion

Publication details, including instructions for authors and subscription information:

<http://www.informaworld.com/smpp/title~content=t713453635>

Shear-Induced Fracture at the Interface of PDMS and a Rigid Slab Modified with Polyelectrolyte Layers

K. H. Kim^a; M. K. Chaudhury^a

^a Department of Chemical Engineering, Lehigh University, Bethlehem, PA, USA

Online publication date: 12 November 2009

To cite this Article Kim, K. H. and Chaudhury, M. K.(2009) 'Shear-Induced Fracture at the Interface of PDMS and a Rigid Slab Modified with Polyelectrolyte Layers', *The Journal of Adhesion*, 85: 11, 792 – 811

To link to this Article: DOI: 10.1080/00218460903291387

URL: <http://dx.doi.org/10.1080/00218460903291387>

PLEASE SCROLL DOWN FOR ARTICLE

Full terms and conditions of use: <http://www.informaworld.com/terms-and-conditions-of-access.pdf>

This article may be used for research, teaching and private study purposes. Any substantial or systematic reproduction, re-distribution, re-selling, loan or sub-licensing, systematic supply or distribution in any form to anyone is expressly forbidden.

The publisher does not give any warranty express or implied or make any representation that the contents will be complete or accurate or up to date. The accuracy of any instructions, formulae and drug doses should be independently verified with primary sources. The publisher shall not be liable for any loss, actions, claims, proceedings, demand or costs or damages whatsoever or howsoever caused arising directly or indirectly in connection with or arising out of the use of this material.

Shear-Induced Fracture at the Interface of PDMS and a Rigid Slab Modified with Polyelectrolyte Layers

K. H. Kim and M. K. Chaudhury

Department of Chemical Engineering, Lehigh University,
Bethlehem, PA, USA

We studied the interaction between a surface modified glass prism and a thin film of PDMS (polydimethylsiloxane) elastomer using a shear adhesion test. The glass prism was chemically modified either by depositing a self-assembled silane monolayer (silanization) or by depositing a few layers of polyelectrolytes. The PDMS was modified only with the polyelectrolyte layers (PEL). While the interaction between the chemically modified glass prism and unmodified PDMS (free of any filler additive) is primarily dispersive, some specific interaction prevails when the PEL-modified glass prism contacts a commercial PDMS (i.e., Sylgard[®] 184) that has silica additives. The surfaces were examined with wettability analysis, atomic force microscopy (AFM), and X-ray photoelectron spectroscopy (XPS) that established the locus of failure. Water immersion tests show that the adhesion between PDMS and glass is stable under water for a long time when the interfacial interaction is mainly dispersive, whereas it deteriorates rapidly when the interface has a polar character.

Keywords: Adhesion; Biofouling; Fracture; Polyelectrolyte; Under water test

INTRODUCTION

When a rigid stud is pulled from a thin elastomeric film bonded to another rigid support, the pull-off stress strongly depends on the modulus and the thickness of the film [1–10]. The adhesive failure is usually accompanied by numerous interfacial bubbles that result from an elastic instability at the interface as described in References [2–15].

Received 30 March 2009; in final form 6 June 2009.

One of a Collection of papers honoring J. Herbert Waite, the recipient in February 2009 of *The Adhesion Society Award for Excellence in Adhesion Science, Sponsored by 3M*.

Address correspondence to M. K. Chaudhury, Department of Chemical Engineering, Iacocca Hall, 11 Research Drive, Lehigh University, Bethlehem, PA 18015, USA. E-mail: mkc4@lehigh.edu

The initial size of these bubbles scales [2,6,8,9,14] with the thickness of the elastomeric film. Beyond a critical stress, the bubbles grow and propagate like cracks, and the stud then disjoins from the elastomeric film. The removal stress [2,5] (σ_n^*) increases with the interfacial work of adhesion (W_a) and the shear modulus (μ) of the film but decreases with the film thickness (h) as follows: $\sigma_n^* \sim \sqrt{W_a \mu / h}$. Recently, the previous study of normal pull-off was extended to a shear-induced release of a rectangular prism from thin confined elastomeric films. It was observed that the critical shear stress [9] at which the prism is released varies as $\sigma_s^* \sim \sqrt{W_a \mu / h}$. In these studies, two other length scales, the length (a) of the prism and the distance (ℓ) between the point of application of the force and the interface, become important:

$$\sigma_s^* \sim \left(\frac{a}{\ell}\right) \sqrt{\frac{W_a \mu}{h}}. \quad (1)$$

The above model was extensively tested [9] in a recent study by varying the aspect ratio (a/ℓ), film thickness, and the shear modulus of a soft elastomeric film. The cases studied by us previously were those where the adhesion was governed by dispersion forces, which was achieved by modifying the surface of the glass with a self-assembled monolayer of alkylsiloxane (decyltrichlorosilane; Gelest Inc., Morrisville, PA, USA). Thus, these previous tests focused primarily on the material and geometric properties of the system. Motivated by the previous observations, we now study a deeper question of adhesion, namely, how does adhesion depend on surface chemistry? The present study is specific to PDMS (polydimethylsiloxane) elastomers, which are currently being investigated as possible easy-release coatings for biofouling [14] applications. Here, minimization of the adhesion of the polymer to different proteinaceous adhesives and the easy release of the latter are key issues. In this application, one of the questions that should be answered is if PDMS participates in polar interactions with another surface.

In order to examine the effect of the polar interactions (Fig. 1) on the work of adhesion, the adhering surfaces were modified with polyelectrolyte layers (PEL) by successive deposition of polycations and polyanions [16–22]. Poly(allylamine hydrochloride) (PAH) and poly(acrylic acid) (PAA) were selected as the polyelectrolyte pair. In a recent paper, Johansson *et al.* [22] studied the adhesion of polyelectrolyte layers using atomic force microscopy (under wet conditions) and the surface force apparatus (under humid and dry conditions) as a function of layer thickness, contact time, and the molecular weight of the polymers. There are several important findings reported in this

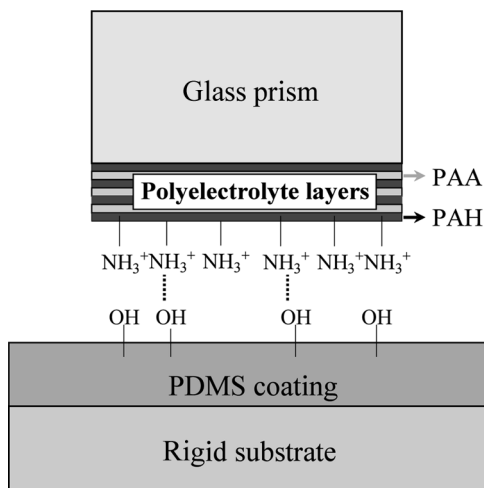


FIGURE 1 Schematic of polyelectrolyte layer (PEL) fabricated system. A few residual hydroxyl groups of the PDMS coating (e.g., Sylgard 184, Dow Corning) can form some weak hydrogen bonds with $-\text{NH}_3^+$ groups of poly(allylamine hydrochloride) (PAH) terminated PEL.

work, such as the increased adhesion with contact time and the number of polyelectrolyte layers. The conclusion of that report is that adhesion is controlled by some kind of inter-digitation of the apposing polyelectrolyte layers. In contrast to the above report, and others cited by Johansson *et al.*, most of our studies were performed with dried polyelectrolytes with a fixed contact time, at a constant ambient condition, and with fixed numbers of polymer layers. Our interest here is not to study the adhesion between two polyelectrolyte layers, but to use these layers to bind to PDMS and a glass substrate. The fracture actually occurs at the polyelectrolyte layer-PDMS interface when an external force is applied. In contrast to the previous report, we do not expect that any significant polymer chain digitation occurs at the PDMS/polyelectrolytes interphase as these polymers are highly incompatible to each other. The adhesion, in our case, should be controlled by thermodynamic work of adhesion. We, thus, do not expect a strong dependence of the adhesion on the polyelectrolyte layer thickness, although this conjecture has not been directly verified experimentally at present. We also studied adhesion under water that produced results different from that in air. These polyelectrolyte components bear some remote resemblances to the amino and carboxylic acid functional groups of natural adhesive proteins, which

may be relevant to understanding the adhesion of fouling organisms to soft elastomeric film.

EXPERIMENTS

The polar interaction was manipulated with the use of the PEL fabrication at the prism/film interface as follows. Two kinds of polyelectrolytes, the cationic poly(allylaminehydrochloride) (PAH, $M_w = 70000$; Aldrich, St. Louis, MO, USA) and the anionic poly(acrylic acid) (PAA, $M_w = 90000$; Polysciences Inc., Warrington, PA, USA) were employed to create the multilayer. The concentration of PAH and PAA was 0.02 M (based on the molecular weight of the repeat unit). PEL was fabricated by submerging the substrate in a PAH bath for 3 min followed by three dippings into fresh deionized (DI) water for 1 min each as a rinsing step. The subsequent layer was formed by submerging the PAH-treated substrate in a PAA bath for 3 min followed by another three-step rinsing cycle. The pH of both the PAH and PAA solutions was adjusted to 3.0 as, at this pH, the deposited PEL layers are known to exhibit a smooth topography [21]. This procedure was repeated until the desired thickness of PAH-PAA layer was achieved on the surfaces [16]. Laboratory synthesized ideal PDMS elastomers ($\mu = 0.9$ MPa) that are free of any fillers as well as commercial PDMS (Sylgard[®] 184, $\mu = 0.75$ MPa; Dow Corning Corp., Midland, MI, USA) were selected as model systems. In these studies, Sylgard 184 provides a good contrast to an ideal network as it possesses some hydroxyl groups on the surface owing to the presence of silica resin as a reinforcement agent. These $-OH$ groups can interact with the $-NH_3^+$ groups of the PAH-terminated PEL as illustrated in Fig. 1. The influence of this additional polar interaction by hydrogen bonding at the interface between the PEL coated glass prism and the PDMS was examined through the shear-induced fracture experiments as described below.

Three polyelectrolyte bilayers were assembled (each bilayer consists of one layer of cationic PAH and another layer of anionic PAA) onto the PDMS film. The uppermost layer of PEL on the PDMS film was treated with another cationic PAH layer. The glass prism, which was adhered to and slid on the PEL-assembled PDMS film, was modified with three polyelectrolyte bilayers. The anionic PAA layer was introduced at the uppermost layer of PEL on the glass prism to bond electrostatically to the cationic PAH terminating layer of PEL on the PDMS. The estimated thickness of five polyelectrolyte bilayers is about $180 \pm 10 \text{ \AA}$, which was inferred from the ellipsometric measurements [Model AutoEL III Ellipsometer, fixed wavelength HeNe

laser ($\lambda = 632.8$ nm) and 70° angle of incidence; Rudolph Technologies Inc., Flanders, NJ, USA] of the thickness of an equivalent layer on a polished silicon wafer. The thickness of one bilayer is, thus, estimated to be ~ 36 Å.

The PEL assembled prism (terminated with an anionic PAA top-layer) was adhered to and sheared against (Fig. 2) a thin PDMS-coated glass slide, the surface of which was modified, as mentioned above, with a PEL but terminated with a cationic PAH top-layer. Because of the weakest adhesive link between PEL and PDMS, the failure is expected to occur at the PEL/PDMS interface, which was indeed confirmed by the studies of atomic force microscopy (AFM, model Nanoscope III; Digital Instruments, Santa Barbara, CA, USA) and X-ray photoelectron spectroscopy (XPS, model Scienta ESCA-300; VG Scienta Inc., Uppsala, Sweden). Simple rinsing of the PDMS with water at the end of the test produces a rectangular

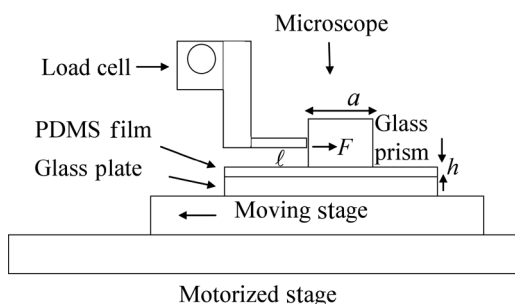


FIGURE 2 Schematic of the shear experiment. A PEL-assembled glass prism ($10 \times 10 \times 6$ mm) is adhered to and then slid on a PEL-coated thin PDMS film bonded to a glass plate. The glass plate is placed on a moving stage, the velocity of which is controlled by a motion controller and computer. The motorized stage is the Nanostep Motorized System (model #17NST103; Melles Griot Inc., Carlsbad, CA, USA). A firmly held beam load cell (model LBB300; Futek Advanced Sensor Technology Inc., Irvine, CA, USA) connected with computer assisted data-acquisition system (model NI USB-9215A; National Instruments Corp., Austin, TX, USA) is used to measure and record the shear force. Sliding is observed with the microscope (model CFM-2 Microscope Video Lenses; Infinity Photo-Optical Company, Boulder, CO, USA) using either a CCD camera (model KP-D20BU; Hitachi, Tokyo, Japan) with a video recorder or high speed camera (model MotionPro; Redlake MASD Inc., San Diego, CA, USA) with a computer. A sharp edge made of aluminum protrudes from the load cell, which makes contact with the glass prism at 1 mm above the interface of contact. As the stage moves, the prism exerts a force on the sharp edge, which is recorded by a load cell and a computer. This figure and the related description are adapted from reference [9].

pattern, the center of which is dewetted, but its surrounding is wetted by water as the PEL is removed from the center and not from the surroundings.

The experiment can also be performed by depositing all of the PEL directly on the glass prism and shearing it against PDMS. We have done such an experiment as well and found that the shear stress in this case is exactly the same as that obtained by the other method. However, in this second method, the wetting-induced pattern formation could not be used as a quick check for interfacial failure. We, thus, opted for the former method in all the tests.

After carefully placing a PEL-modified glass prism ($10 \times 10 \times 6$ mm) on a PEL-assembled PDMS film, we waited for an hour before performing the shear experiments. The glass prism was sheared against the PDMS by applying a force at a height of 1 mm above the interface (Fig. 2). The force was measured with a beam load cell (model LBB300; Futek Advanced Sensor Technology Inc., Irvine, CA, USA). The substrate was translated horizontally at various speeds using a motorized stage and a motion controller (model #17NST103; Melles Griot Inc., Carlsbad, CA, USA) operated by a computer. The velocity was increased incrementally (0.002 mm/s for 2 sec) in a stepwise manner until the prism completely separated from the film. Some of the adhesion studies were also conducted by pre-adsorbing a natural adhesive protein [from *Mytilus edulis* (blue mussel), $M_w \sim 130,000$, composed of 75–85 repeated sequences of hexa- and decapeptides, Cat. No. A2707; Sigma-Aldrich, St. Louis, MO, USA] on PDMS. The adhesion force measurements with these proteins were conducted in air as well as in water using the shear force apparatus described above. More details of these measurements are given below.

RESULTS AND DISCUSSION

The Effect of Interfacial Interaction on Shear-Induced Fracture

Let us first briefly summarize the mechanism of shear-induced release of a glass prism from a thin confined film of PDMS, the details of which have been described in an earlier publication [9]. When a prism is made to slide on the PDMS coating, a frictional force develops at the interface that increases with the sliding velocity. This frictional force itself does not lead to fracture. However, as the friction force and the external force (this is actually a reaction force) creates a torque, it tilts the prism slightly. As can be expected, the magnitude of this torque is proportional to the frictional stress, which increases with the sliding

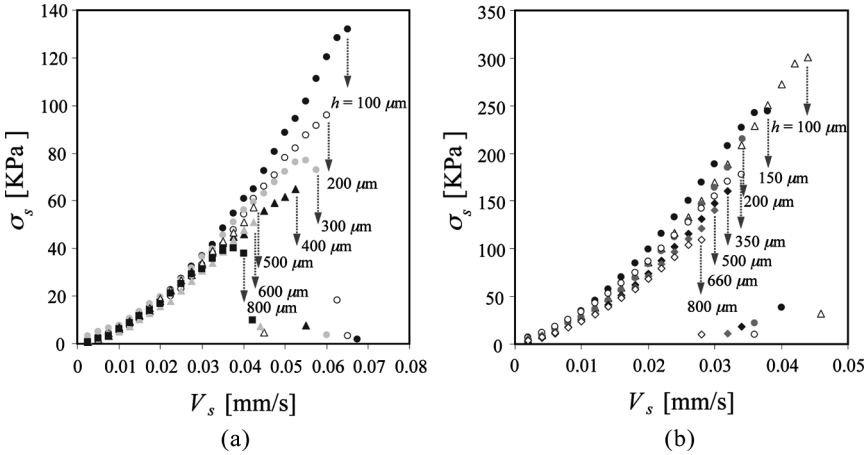


FIGURE 3 Shear stress (σ_s) of a silanized glass prism on Sylgard 184 (Fig. 3a) and a PEL-assembled glass prism sliding against PEL-coated Sylgard 184 as a function of thickness (Fig. 3b). The locus of a specific symbol represent the shear stress transmitted at the interface of the prism and the substrate at different sliding velocities. Arrows represent the critical shear stress (σ_s^*) at which the prism comes off the film. The figure shows that the critical shear force decreases with the increase of film thickness.

velocity. If this torque is small due to low friction, as is the case with elastomers of low crosslink density, the prism continues to slide on the PDMS film without ever coming off. However, as the sliding velocity is increased, the torque also increases until it reaches the critical value at which the prism is separated from the PDMS coating. This ultimate critical stress to fracture decreases with the increase of the film thickness (Fig. 3), as expected from Eq. (1). As the PDMS films used in these experiments are quite thin and confined, the viscoelastic dissipation is negligible in the bulk of the film. The friction increases with the inter-crosslink density, *i.e.*, with the decrease of the molecular weight of the polymer—a trend that is opposite to that expected of the shear fracture being controlled by the viscoelastic deformation in the film.

Interaction of PEL with Ideal Network PDMS and Sylgard 184

We first present the results of the shear fracture experiments with an ideal PDMS network, which does not contain any hydroxyl groups on the surface. The Si2P region of the X-ray photoelectron spectrum of

such a network has only one peak at 102 eV that corresponds to the silicon of dimethyl siloxane network (Fig. 4). To provide a contrast, the Si2P region of a commercial PDMS (Sylgard 184) is also shown in Fig. 4 that shows a tail. This spectrum can be decomposed into two peaks, one at 102 eV and the other at 103 eV, indicating the presence of oxidized silicon, which arises, presumably, from the silica resin present in the network. This resin, being close to the PDMS/air interface, can potentially engage in specific interaction with another surface.

Figure 5 summarizes the critical shear stresses of a glass prism against an ideal network PDMS ($\mu = 0.9$ MPa) under two different conditions. When the glass prism is silanized and it interacts with the unmodified ideal networks, the interaction is *via* a low energy dispersion interaction. However, when both the glass prism and the PDMS are modified with PEL of opposite polarity, fracture occurs at the PEL/PDMS interface. In both the cases, the critical shear stress of fracture varies with thickness as $h^{-0.5}$. Using the typical value of the work of adhesion for the silanized glass prism interacting with PDMS as ~ 40 mJ/m², the work of adhesion between the PEL and the PDMS is estimated to be 63 mJ/m² using Eq. (1). Since the dispersion component of the surface energy of PEL is in the range of 40 mJ/m² and that of PDMS is 20 mJ/m², we expect the work of adhesion between PEL and PDMS to be about 56 mJ/m² using the geometric mean approximation of the work of adhesion. This work of adhesion is close to the value (63 mJ/m²) found experimentally. Thus, we believe that there is minimum polar interaction between the PEL and an ideal PDMS network. The situation is, however, different with

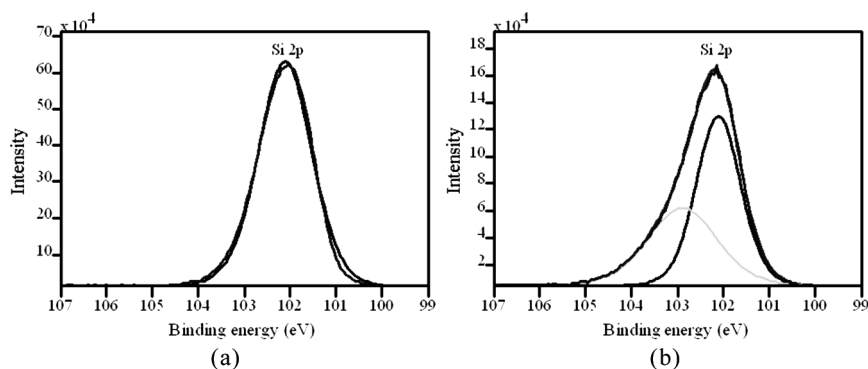


FIGURE 4 X-ray photoelectron spectrum of the Si 2P region of an ideal network (a) and Sylgard 184 (b).

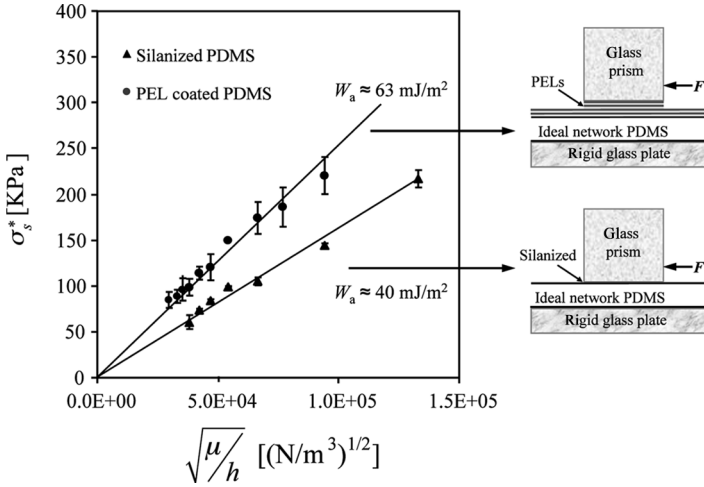


FIGURE 5 Shear induced fracture at the interface of an ideal PDMS network against two surfaces: a silanized glass prism and polyelectrolyte layer coated glass prism. In these experiments only the thickness of the PDMS film was varied. However, the data are plotted against $\sqrt{\mu/h}$ so that the results obtained with polymers of differing modulus can be compared.

Sylgard 184, where the OH groups of silica resin can produce hydrogen bonds with NH_3^+ of the PAH layer-terminated PEL. This picture is consistent with the higher work of adhesion value (110 mJ/m^2) that is found for the Sylgard 184/PEL interface (Fig. 6).

In order to strengthen our argument regarding the possible role of H-bonding interactions, the surface of PDMS was hydrolyzed which is expected to increase the number of hydroxyl groups on the surface. The hydrolyzed PDMS films were prepared [23] by immersing PDMS film in a dilute solution of hydrochloric acid ($\text{pH} \sim 1.7$) overnight. The PDMS films were then washed in DI water, dried with nitrogen and stored under a low vacuum. Table 1 summarizes the water contact angles of Sylgard 184 before and after hydrolysis. Since the concentration of the $-\text{OH}$ groups supposedly increases due to hydrolysis [23], the contact angle values on hydrolyzed PDMS were slightly smaller than those on un-hydrolyzed polymer.

Figure 6 summarizes the critical shear stresses of the hydrolyzed and the PEL-assembled Sylgard 184, which are also compared with a control where only dispersion interaction prevails. In all cases, the critical shear stress varies with film thickness as $\sigma_s^* \sim h^{-0.5}$. The work of adhesion for the hydrolyzed and PEL-assembled PDMS is estimated to be

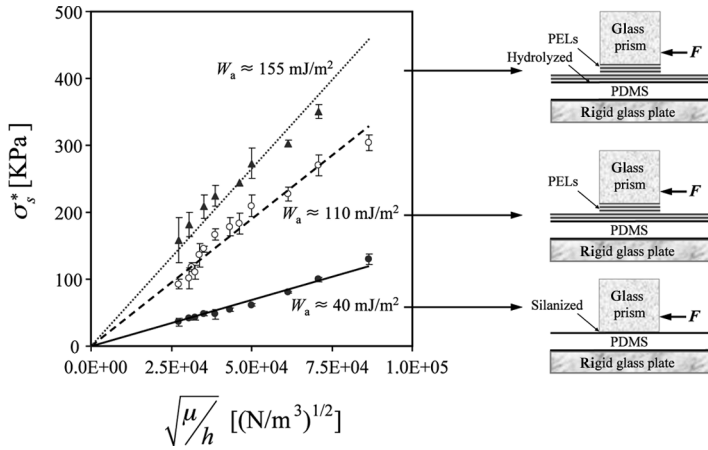


FIGURE 6 Shear induced fracture at the interface of Sylgard 184 against two surfaces: a silanized glass prism and a polyelectrolyte layer. In these experiments, as with those reported in Fig. 5, only the thickness of the PDMS film was varied. However, the results are shown against $\sqrt{\mu/h}$ so that results obtained with polymers of differing modulus can be compared. In this figure an additional set of data is provided with a hydrolyzed Sylgard 184.

approximately 155 mJ/m^2 using Eq. (1), in contrast to the value of the dispersion interaction on the hydrocarbon surface ($W_a \sim 40 \text{ mJ/m}^2$) [6]. A somewhat similar effect was previously reported in References [22,23] using the contact mechanics test.

Interaction Between an Adhesive Protein and Sylgard 184

The natural adhesive protein [24] was also employed as a surface modifier to mimic, somewhat crudely, a practical situation of biofouling on a soft elastomeric coating. The protein, which contains amino functional groups, was adsorbed as a first layer on Sylgard[®] 184. The existence of the adsorbed first protein layer was proven by the presence of nitrogen in X-ray photoelectron spectroscopy (XPS). The polyanions (PAA) and the polycations (PAH) layers were then consecutively adsorbed on

TABLE 1 Advancing and Receding Contact Angle Values for Sylgard 184 and its Hydrolyzed Version

	PDMS	Hydrolyzed PDMS
Advancing	$\sim 113^\circ$	$\sim 87^\circ$
Receding	$\sim 100^\circ$	$\sim 70^\circ$

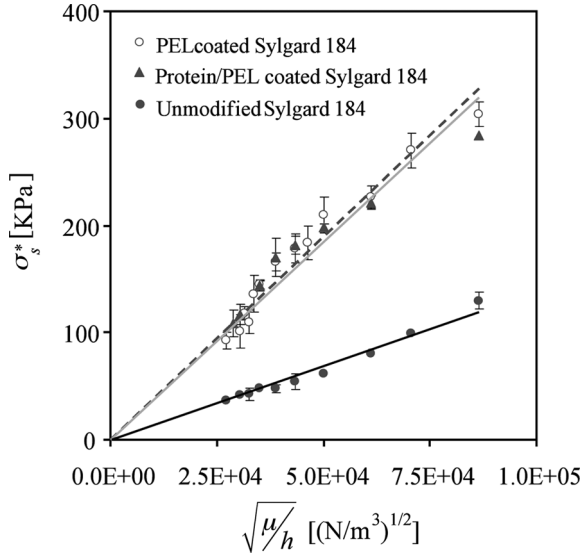


FIGURE 7 The comparison of critical shear stresses (σ_s^*) on a PEL-assembled Sylgard 184 [open circles (\circ), $W_a \sim 110 \text{ mJ/m}^2$] and with natural adhesive protein deposited on Sylgard 184 [black triangle (\blacktriangle), $W_a \sim 108 \text{ mJ/m}^2$]. Black circles (\bullet) represent critical shear stresses (σ_s^*) of a silanized glass prism on chemically unmodified Sylgard 184 films ($W_a \sim 40 \text{ mJ/m}^2$). The dashed, grey, and black lines indicate the least square fits of the data for the open circles, black triangles, and black circles, respectively.

the surface, assuming that the shear-induced adhesive failure would take place at the PDMS/protein interface.

PEL layers were assembled onto protein-adsorbed Sylgard 184 and the shear fracture experiment was carried out with another PEL-modified glass prism as discussed above. The critical shear stress of the proteineous adhesive-treated PDMS is nearly the same as that of the PEL-assembled PDMS (Fig. 7). Therefore, the use of polyelectrolyte components, *i.e.*, PAH and PAA, not only bears the resemblance to the adhesive proteins, but also is highly relevant in understanding the adhesion of fouling organisms to soft elastomeric coatings. The characterization of the fracture location is discussed in the following section.

Characterization of the Fracture Location

After every shear experiment, deionized water was sprayed on its surface. In all cases, the region of the PDMS, where the glass prism was contacted and slid, was not wetted by water. But full wetting

was observed in the surrounding region. The observation suggests that polyelectrolyte is removed from the PDMS surface by the shear force. In other words, the shear-induced fracture takes place at the PEL/PDMS interface. AFM and XPS analysis were performed to further verify the location of the shear-induced fracture of the PEL-assembled PDMS. The results of both analyses are reported below.

AFM Studies on PDMS before and after the Shear Test

Figure 8 presents a comparison of the AFM topographic images of the Sylgard 184 and an ideal PDMS surface, on which adhesion experiments were conducted with PEL. The surfaces appear to be

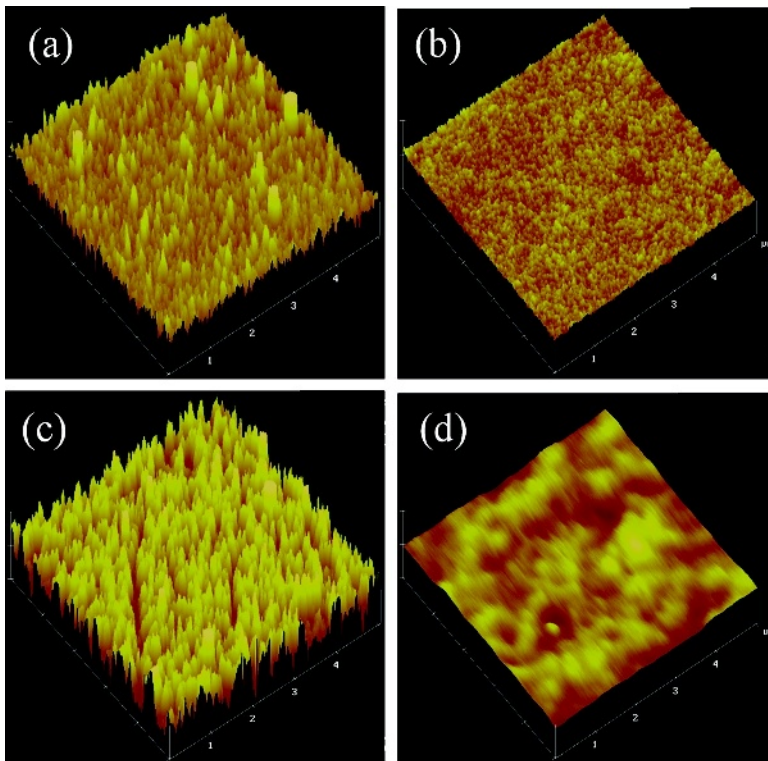


FIGURE 8 AFM images of PEL-fabricated Sylgard 184 (a) before and (b) after fracture as well as PEL-assembled ideal PDMS network (c) before and (d) after fracture tests. These represent the regions where the prism was contacted and slid. Length scale is 5 micrometers and depth scale is 10 nanometers in AFM images.

TABLE 2 Root Mean Squared (RMS) Roughness Values for Both Only PEL-Fabricated and Hydrolyzed and PEL Assembled PDMS Calculated from AFM Imaging. The Values of After Experiments are Obtained from the Region at Which the Prism was in Contact and Slid. In the last column, the Range 0.6 to 2.6 nm Indicates a Heterogeneous Fracture

	PEL before exp.	PEL after exp.	HCl/PEL before exp.	HCl/PEL after exp.
Sylgard 184	2.1 nm	0.4 nm	4.3 nm	0.6 to 2.6 nm
Ideal network PDMS	3.8 nm	0.4 nm	.	.

somewhat rough in the beginning when PEL is deposited on its surface. After the shear experiments, the topographical images of the surfaces [Figs. 8(b) and (d)] become much smoother indicating that most of the PEL has been removed.

Table 2 summarizes the results of root mean squared (RMS) roughness of these surfaces as obtained from the AFM images. The roughness values on the PEL-assembled PDMS, including the hydrolyzed/PEL fabricated PDMS, are much greater than those on the region where the prism is contacted and slid, *i.e.*, after the shear experiment, are shown in Table 2.

These AFM results correspond well with the results of the DI water wettability test that shows that the region where the prism is sheared does not wet after the shear experiment. This implies the removal of hydrophilic PEL, thus exposing the hydrophobic PDMS underneath. The shear-induced fracture, therefore, occurs at the PEL and PDMS interface. For the hydrolyzed Sylgard 184, the domain of the fracture region has a low roughness value (0.6 nm) but some occasional points in that region have a relatively high value (2.6 nm) of roughness indicating that heterogeneous fracture occurs on some scattered spots.

XPS Studies on PDMS Before and After the Shear Test

XPS analysis was also performed to examine the location of the fracture at the interface. We first present the results obtained with an adhesive protein, where an XPS peak for nitrogen (~ 400 eV) can be caused by either the amino group of the adhesive protein (before the test) or due to the protein or the $-\text{NH}_3^+$ functional group of PEL after the fracture test if clean interfacial failure does not occur. The extent of nitrogen present was measured before and after fracture. An experimental difficulty arises due to the low signal-to-noise ratio which can usually

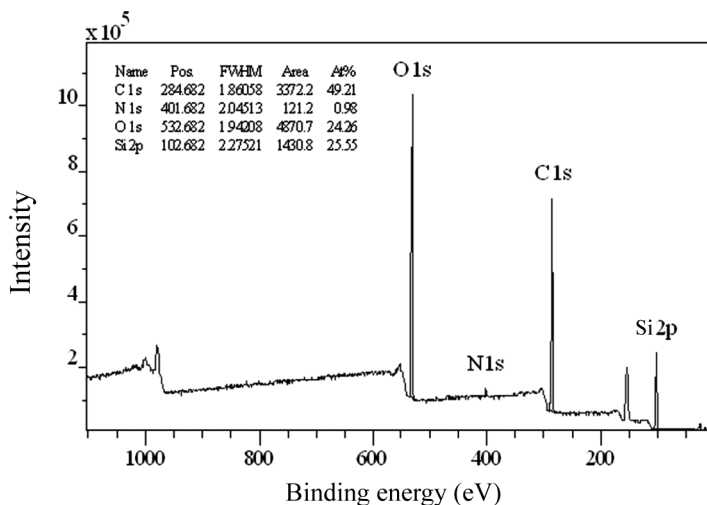


FIGURE 9 XPS results of the adhesive protein layer adsorbed on Sylgard 184 before further PEL assembly and fracture tests. The atomic percentage of nitrogen (N1s, ~ 400 eV) is about 1%.

be circumvented with accumulated scans. Even then, the nitrogen only registers as a small peak because of its relatively low scattering cross-section. Figure 9 presents the XPS results of the adhesive protein layer adsorbed on the Sylgard 184 to illustrate the typical spectra obtained in the study. In this figure, a finite (but small) atomic percentage of the nitrogen peak ($\sim 1\%$) is the evidence of the adsorbed adhesive protein layer on Sylgard 184. After the shear adhesion test, the nitrogen peak disappears, or blends with the background. The nitrogen peak that originates from the PAH layer (Fig. 10a) on an ideal network PDMS decreases considerably (2.29% to almost background value) after the shear-induced fracture test is performed. It again implies that most of the nitrogen was removed in the shear test. The PEL-fabricated Sylgard 184 and its hydrolyzed version were also analyzed by XPS. In all cases, some nitrogen is detected before the fracture test. However, after the shear fracture test, the nitrogen level becomes comparable with the background.

Underwater Adhesion Tests

The method of studying adhesion in air *via* shear fracture as described in this paper can also be used to study adhesion under aqueous medium (Fig. 11) by modifying the experimental facility described in

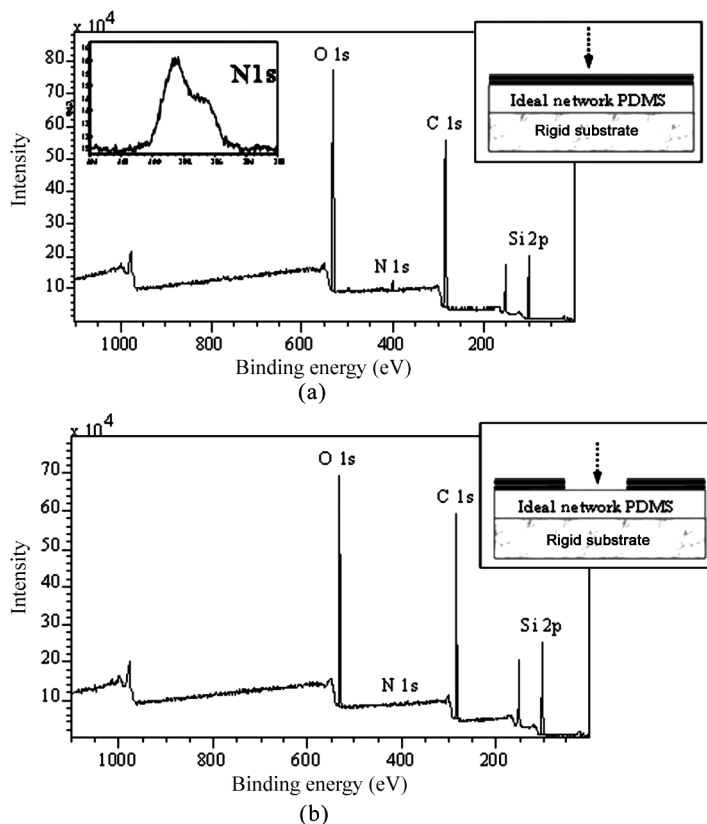


FIGURE 10 XPS results and corresponding schematics (a) before and (b) after the shear experiments of ideal network PDMS on the region in which the prism was contacted and slid. The dotted arrows in the inset figure represent the scanning area.

Fig. 2. The polyelectrolyte layer (PEL)-deposited PDMS substrate is firmly bonded to the base of a miniature water chamber, which is strongly fixed to a motorized stage capable of moving at various speeds. A PEL-modified glass prism is placed on PEL assembled PDMS in air. After waiting for up to 1 hour to ensure intimate contact of the prism with the PDMS interface, the chamber is filled with either DI water or salt water. The pH of DI water and salt water is about 7.0. The level of water in the chamber is at least 5 mm above the upper flat surface of the glass prism. The water chamber is attached to a moving stage, which is adjusted by a motorized stage controlled by both a nano-motion controller system (Model #17NST103; Melles Griot

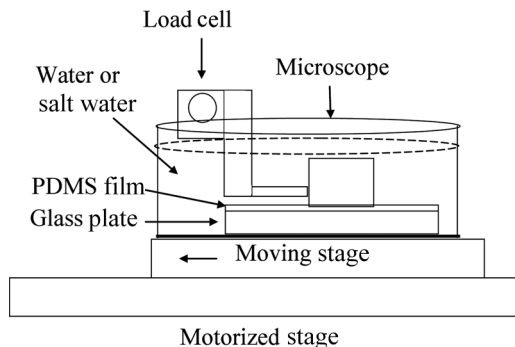


FIGURE 11 Schematic of shear experiment set up (under water condition). PEL assembled prism ($10 \times 10 \times 6$ mm) is placed on a PEL-fabricated PDMS film bonded on glass substrate in a chamber. Then the water chamber is fully filled with distilled or salt water. For other details see the caption of Fig. 2.

Inc., Carlsbad, CA, USA) and a computer. A programmed velocity was used, in which the velocity increased by incremental steps of 0.005 mm/s for the time duration of 2 sec. As the water chamber starts moving, the shear force is transmitted onto the prism and is measured using the method described above.

Figures 12 and 13 summarize the results of the critical shear stresses obtained with Sylgard 184 ($\mu = 0.75$ MPa) and an ideal network ($\mu = 0.9$ MPa) of various thicknesses both in air and under water. As is the case with air, the shear stress followed relationship $\sigma_s \sim h^{-0.5}$ under water as well. No significant difference of adhesion is observed between the distilled and salt water (3.5 wt% of NaCl, Fisher Scientific, Fair Lawn, NJ, USA, in DI water), although a reduction of adhesion under water from that in air is evident. The DI water spreading test was performed after every underwater experiment to verify the location of fracture (PDMS films are dried by nitrogen gas then DI water was spread on the film). In every case, the region in which the glass prism was initially contacted and slid was not wetted, which suggests that most of the polyelectrolytes on PDMS were removed by the shear force, *i.e.*, the shear-induced fracture occurred at the PEL and PDMS interface even under water.

Finally, we report a long-term underwater (salt water) adhesion study that was conducted with the shear fracture method. Here, an adhesive protein is present at the interface of PDMS (Sylgard 184, 400 μm thick) and PEL, for which the adhesion results in air have been summarized previously. The silanized glass against Sylgard 184 was used as a control. Because a silanized glass interacts with PDMS *via*

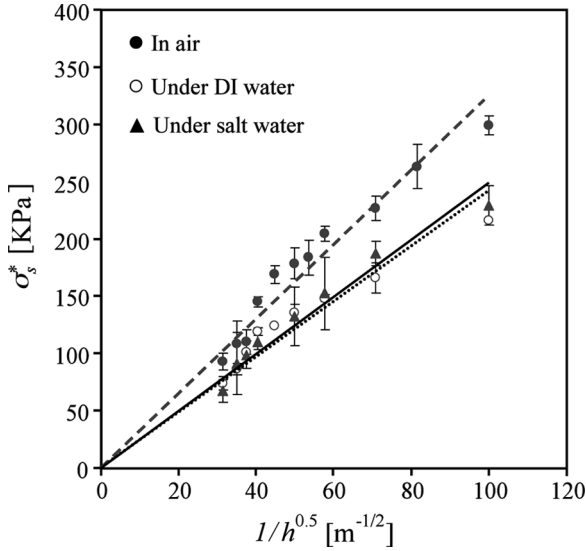


FIGURE 12 Film thickness (h) dependence of critical shear stress on PEL-assembled commercial PDMS (Sylgard 184, $\mu=0.75$ MPa) in air [black circles (●)], under DI water [white circles (○)], and under salt water [black triangles (▲)].

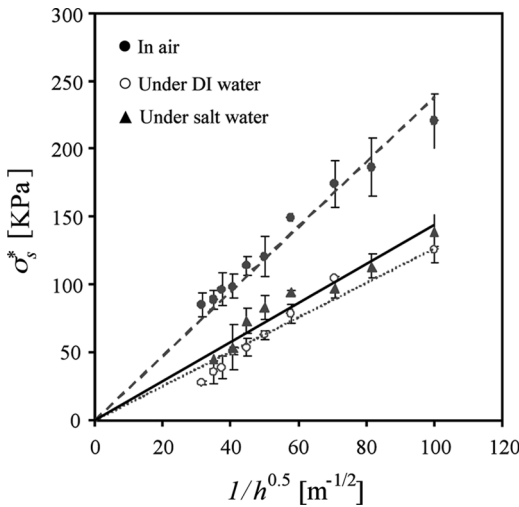


FIGURE 13 Film thickness (h) dependence of critical shear stress on PEL-assembled ideal network PDMS ($\mu=0.9$ MPa) in air [black circles (●)], under DI water [white circles (○)], and under salt water [black triangles (▲)].

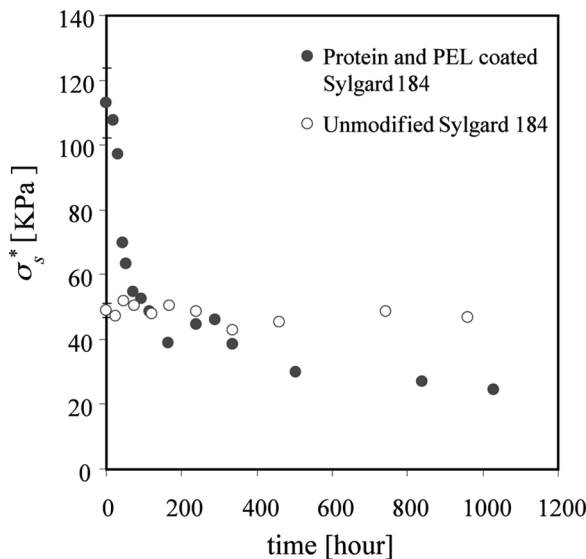


FIGURE 14 Deterioration of adhesion occurs under salt water for polar interface, whereas the non-polar interface is quite stable.

dispersion forces, we do not expect any long-term degradation of this adhesive interface under water. Indeed, the critical shear force for fracture maintains a value of about 50 KPa for about 1000 h of water immersion (Fig. 14). On the other hand, the protein and PEL-modified PDMS (MEFP)/PEL-coated glass show a strong adhesion initially (110 KPa) for a short-term immersion (*i.e.*, 1 h) in water, but this adhesion continued to decrease with time. After 1000 h, the adhesion, in this latter case, decreases to about 20 MPa, which is lower than that for unmodified PDMS against silanized glass. Furthermore, the data exhibit no indication of saturation. It is likely that after a much longer period of time the adhesion would drop to zero. This study indicates that the adhesion of MEFP/PEL-coated glass with PDMS is not stable thermodynamically. The initial strong adhesion achieved through polar interaction is susceptible to decrease through the competitive interaction of the polar moieties with water that diffuses through the interface and weakens the interface.

SUMMARY AND CONCLUSION

An experimental system is described with which the polar interaction between PDMS and a polyelectrolyte multilayer or even an adhesive protein layer can be studied. The system consists of bringing a

PEL-modified PDMS and a PEL-modified glass prism into contact and subsequently shearing them off. In this study, the modulus of the PDMS film was kept constant, whereas its thickness was varied with each type of interaction. In all cases, the shear fracture stress decreased with the film thickness following a square root relationship, which was originally observed for a dispersion interaction [9]. Wettability, AFM, and XPS studies indicate that the fracture takes place at the interface of the PDMS and the counter-surface. Two major conclusions may be drawn from these studies as they are summarized below.

1. The interaction between an ideal PDMS network and a polyelectrolyte layer, where the work of adhesion is about 63 mJ/m^2 , appears to be governed by dispersion interactions.
2. The adhesion between Sylgard 184 and a polyelectrolyte layer, where the work of adhesion is about 110 mJ/m^2 , seems to be contributed by a hydrogen bonding interaction. This H-bonding interaction could be due to the presence of some hydroxyl groups on the surface, which increases further if the surface is hydrolyzed in dilute HCl. Although this H-bonding interaction provides a relatively long-term bonding under water, it slowly deteriorates with time. Water-resistant bonds are provided by the control where dispersion force prevails.

ACKNOWLEDGMENT

This work was supported by the Office of Naval Research (N000140810743 P00001). We thank Jonathan Longley and Chi-Hsiu Lin for carefully reading and correcting the manuscript.

REFERENCES

- [1] Kendall, K., *J. Phys. D: Appl. Phys.*, **4**, 1186–1195 (1971).
- [2] Chung, J. Y. and Chaudhury, M. K., *J. Adhesion* **81**, 1119–1145 (2005).
- [3] Lakrout, H., Sergot, P., and Creton, C., *J. Adhesion* **69**, 307–359 (1999).
- [4] Crosby, A. J., Shull, K. R., Lakrout, H., and Creton, C., *J. Appl. Phys.* **88**, 2956–2966 (2000).
- [5] Chung, J. Y., Kim, K. H., Chaudhury, M. K., Sarkar, J., Sharma, A., *Eur. Phys. J. E* **20**, 47–53 (2006).
- [6] Kim, J., Nyren-Erickson, E., Stafslin, S., Daniels, J., Bahr, J., and Chisholm, B. J., *Biofouling* **24**, 313–319 (2008).
- [7] Webber, R. E., Shull, K. R., Roos, A., and Creton, C., *Phys. Rev. E* **68**, 021805 (2003).
- [8] Ghatak, A. and Chaudhury, M. K., *Langmuir* **19**, 2621–2631 (2003).
- [9] Chaudhury, M. K. and Kim, K. H., *Eur. Phys. J. E* **23**, 175–183 (2007).
- [10] Ghatak, A., *Phys. Rev. E* **73**, 041601 (2006).

- [11] Ghatak, A. and Chaudhury, M. K., *J. Adhesion* **83**, 679–704 (2007).
- [12] Ghatak, A., Chaudhury, M. K., Shenoy, V., and Sharma, A., *Phys. Rev. Lett.* **85**, 4329–4332 (2000).
- [13] Shenoy, V. and Sharma, A., *Phys. Rev. Lett.* **86**, 119–122 (2001).
- [14] Chaudhury, M. K., Finlay, J. A., Chung, J. Y., Callow, M. E., and Callow, J. A., *Biofouling* **21**, 41–48 (2005).
- [15] Mönch, W. and Herminghaus, S., *Europhys. Lett.* **53**, 525–531 (2001).
- [16] Decher, G., *Science* **227**, 1232–1237 (1997).
- [17] Decher, G., Hong, J. D., and Schmitt, J., *Thin Solid Films* **210/211**, 831–835 (1992).
- [18] Wagberg, L. and Kolar, K., *Ber. Bunsen Ges. Phys. Chem. Chem. Phys.* **100**, 984–993 (1996).
- [19] Muller, M., Meier-Haack, J., Schwarz, S., Buchhammer, H. M., Eichhorn, K.-J., Janke, A., Kebler, B., Nagel, J., Oelmann, M., Reihls, T., and Lunkwitz, K., *J. Adhesion* **80**, 521–547 (2004).
- [20] Yoo, D., Shiratori, S. S., and Rubner, M. F., *Macromolecules* **31**, 4039–4318 (1998).
- [21] Shiratori, S. S. and Rubner, M. F., *Macromolecules* **33**, 4213–4219 (2000).
- [22] Johansson, E., Blomberg, E., Lingstrom, R., and Wågberg, L., *Langmuir* **25**, 2887–2894 (2009).
- [23] Chaudhury, M. K., Weaver, T., Hui, C. Y., and Kramer, E. J., *J. Appl. Phys.* **80**, 30–37 (1996).
- [24] Waite, J. H., *J. Biol. Chem.* **258**, 2911–2915 (1983).